

The genomic landscape of cholangiocarcinoma reveals the disruption of post-transcriptional modifiers

Supplementary Figure 1

Supplementary Figure 2

Supplementary Figure 3

Supplementary Figure 4

Supplementary Figure 5

Supplementary Figure 6

Supplementary Figure 7

Supplementary Table 1

Supplementary Table 2

Supplementary Table 3

Supplementary Table 4

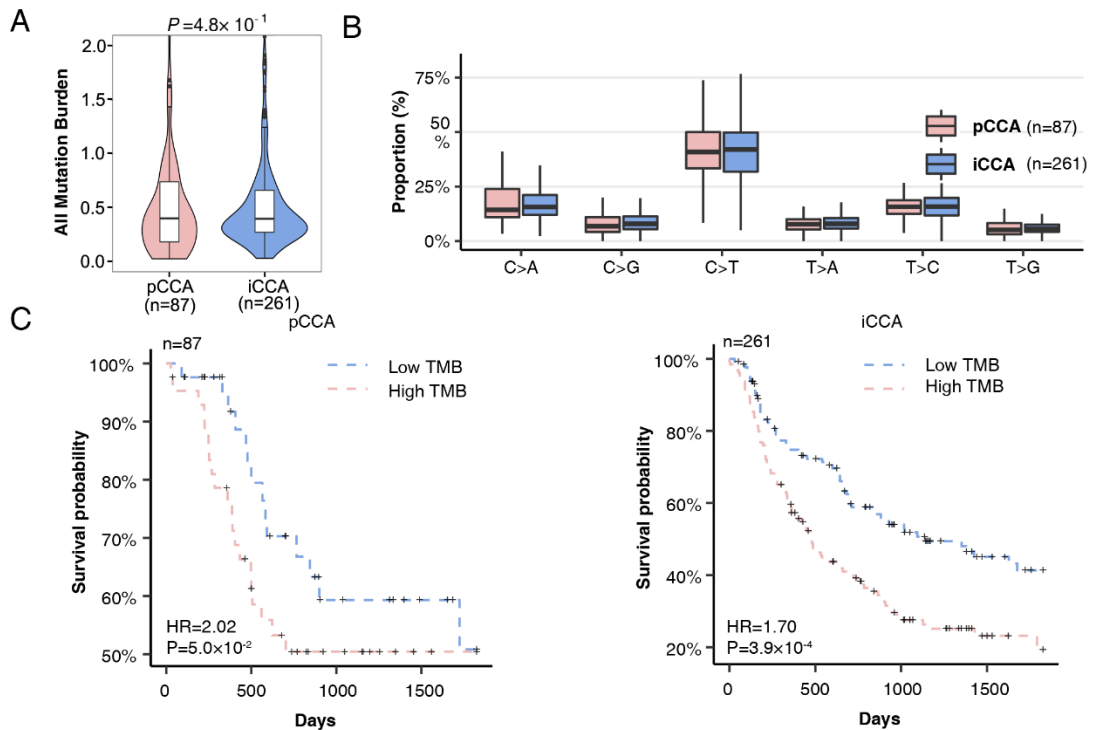
Supplementary Table 5

Supplementary Table 6

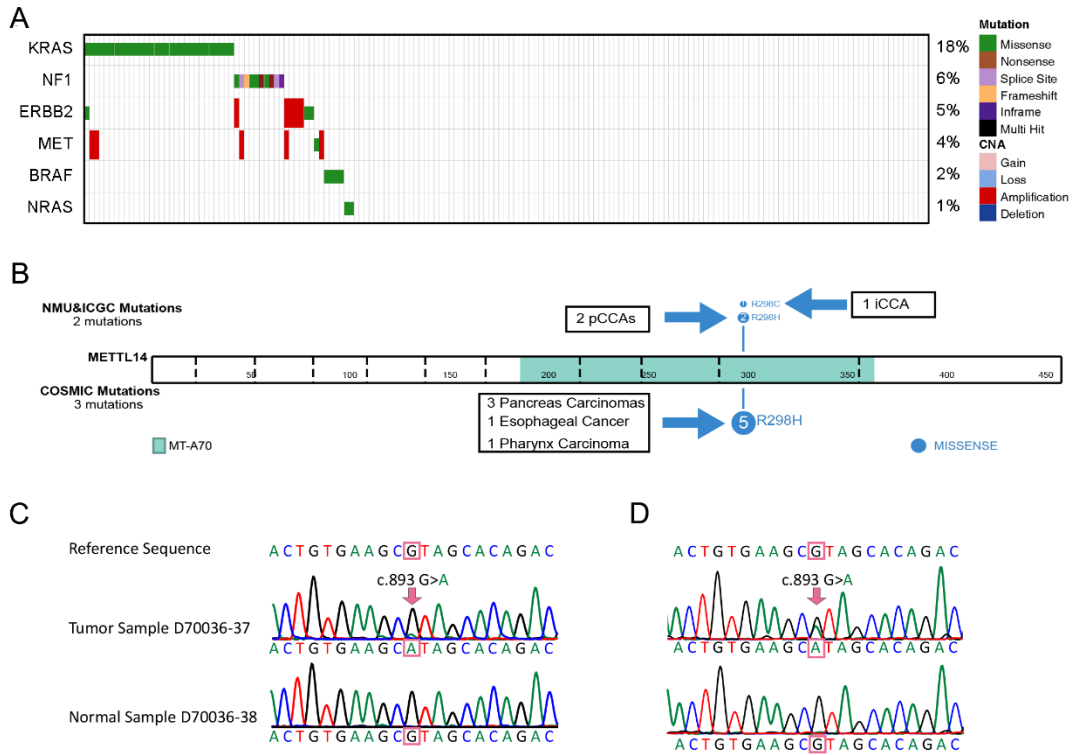
Supplementary Table 7

Supplementary Table 8

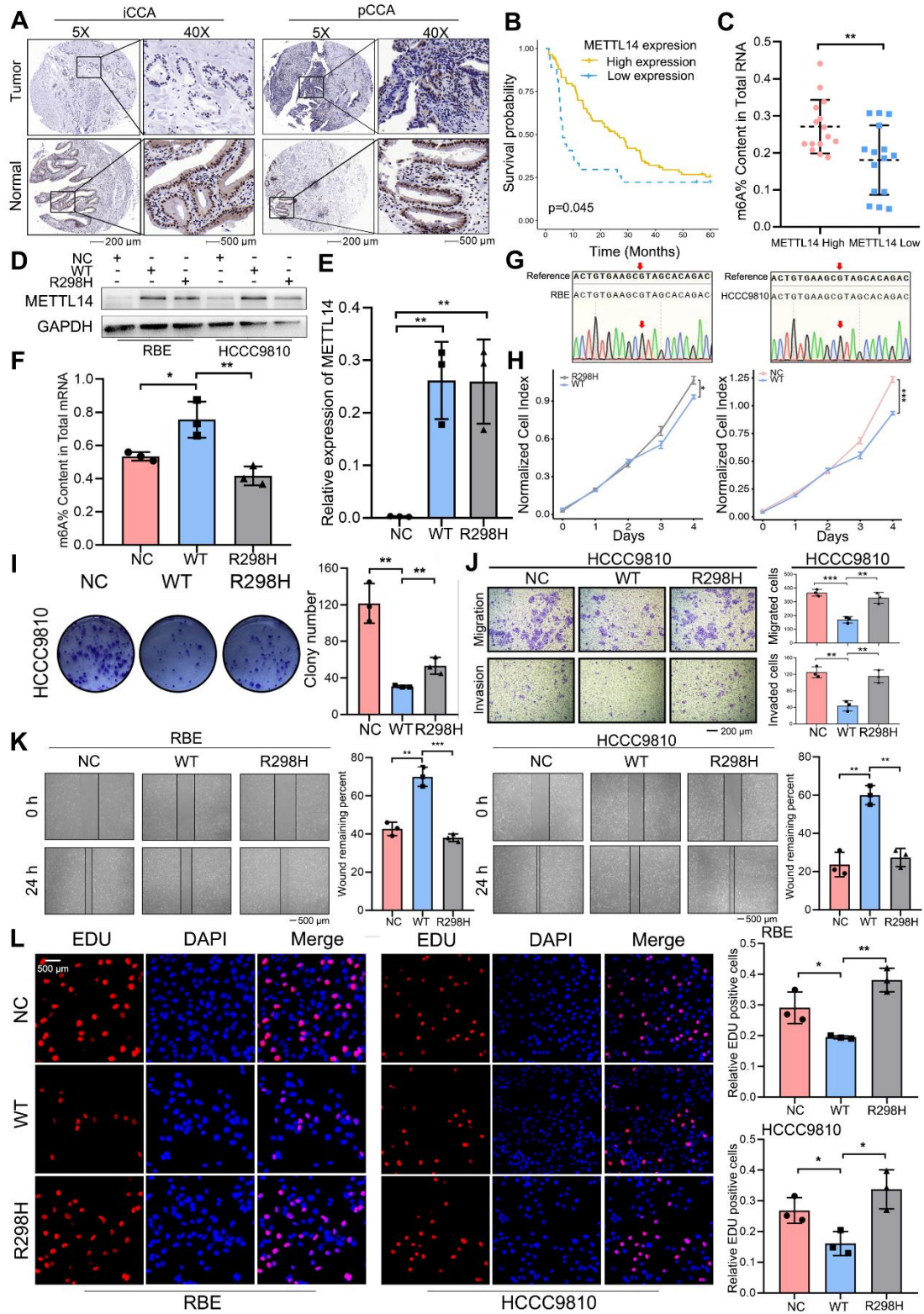
Supplementary Table 9



Supplementary Fig. 1 **(A)** Boxplot of all mutation burden in pCCA and iCCA. Wilcoxon rank-sum test was performed to obtain the P value. **(B)** Constitution of six types of single nucleotide substitutions between iCCAs (presented in blue) and pCCAs (presented in light red). Box plots depicted the median, quartiles and range. The whiskers in box plots extended to the most extreme data point which is no more than 1.5 times IQR. Outliers were identified using upper/lower quartile ± 1.5 times IQR. **(C)** Kaplan-Meier survival plot between iCCA (left panel) and pCCA (right panel) patients with high TMB and low TMB. Cox proportional hazards model adjusted for age, gender, and tumor stage was performed to obtain HR and P values.

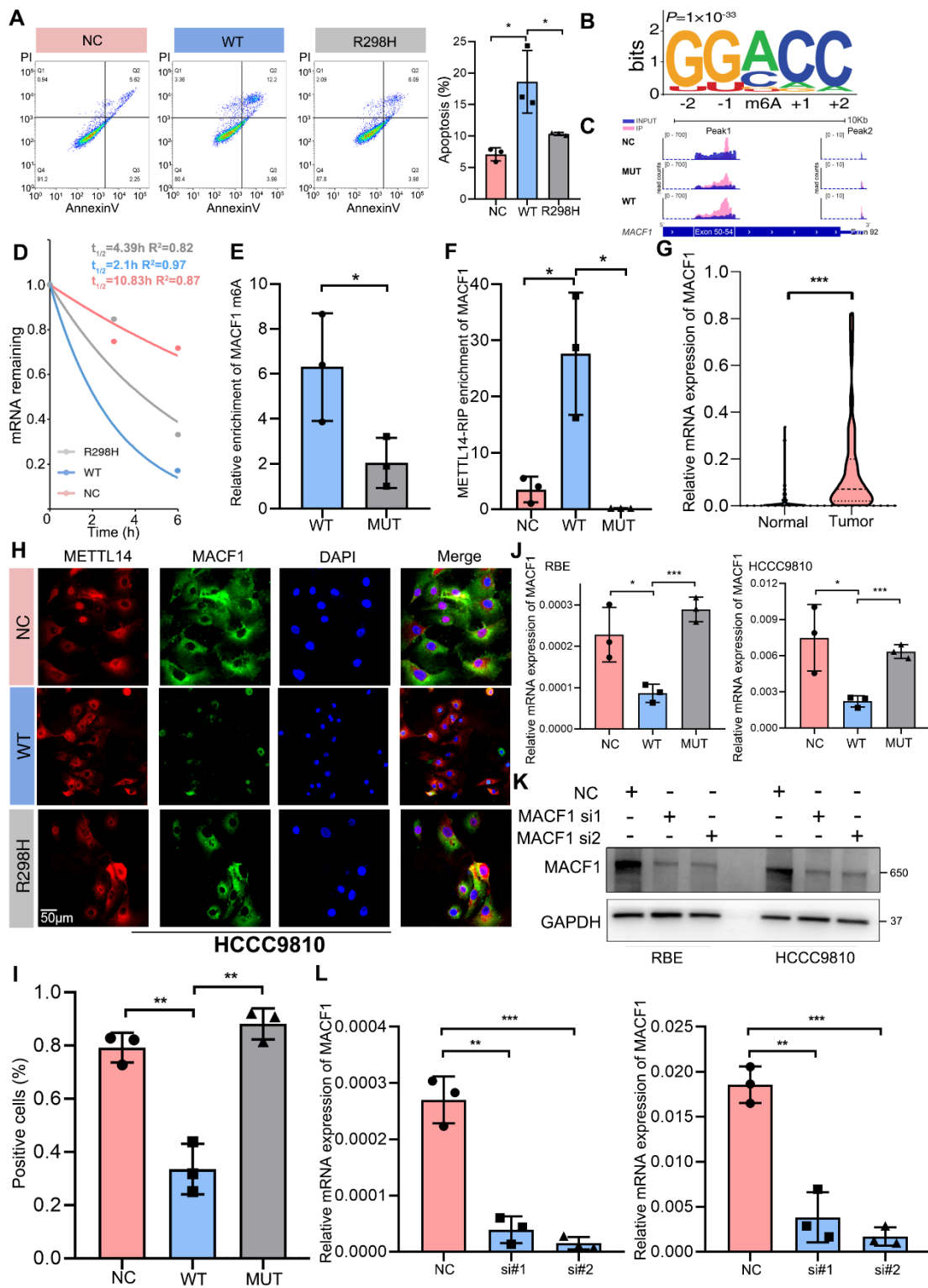


Supplementary Fig.2 **(A)** Characters in CNA and mutation of driver genes in RAS-RTK pathway. **(B)** Lollipopplot of METTL14 R298H and R298C. The top panel represents mutations in this study and the bottom panel represents mutations from COSMIC dataset. **(C & D)** Sanger sequencing plot of interested region including METTL14 R298H of the NMU subject **(C)** and the additional subject **(D)**.



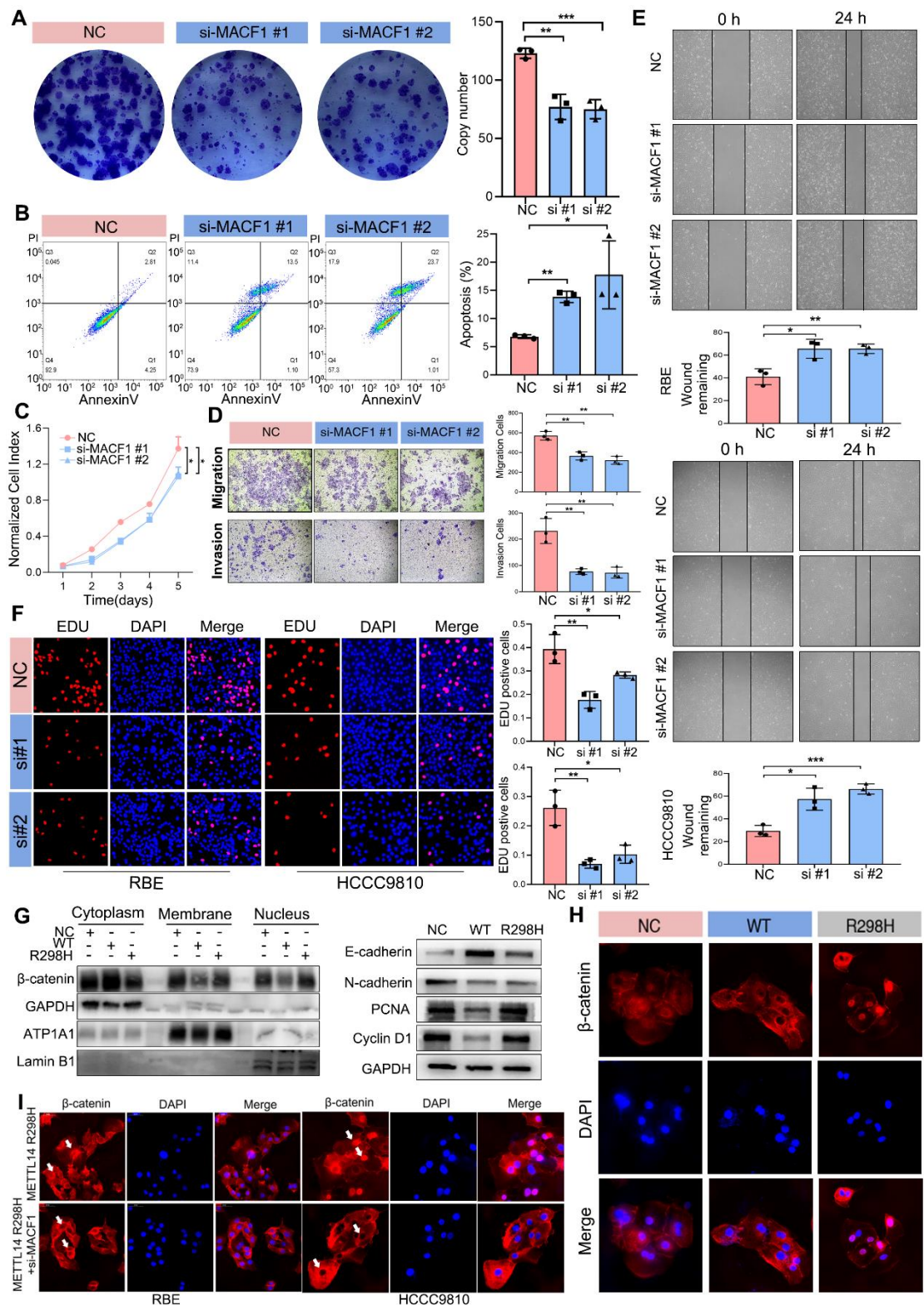
Supplementary Fig.3 (A) Representative IHC stains of METTL14 in iCCA and pCCA tissues and matched adjacent normal tissues. **(B)** METTL14 downregulation in CCA tissues was associated with shorter cancer-specific survival in CCA patients (n=111).

(C) The m⁶A contents of total mRNA in METTL14 High group (n=15) and METTL14 Low group (n=15). **(D)** Stable METTL14^{R298H} and METTL14^{wt} Cells were screened by western blot. **(E)** The transfection efficiency of lentiviral constructs expressing METTL14^{wt} and METTL14^{R298H} in HCCC9810 cell line (n=3). **(F)** METTL14^{R298H} reduced METTL14^{wt}-mediated m⁶A modification detected by m⁶A colorimetric quantification in HCCC9810 cell line (n=3). **(G)** Sanger sequencing plot of interested region including METTL14 R298 of cholangiocarcinoma cell lines (RBE and HCCC9810). **(H)** Proliferation curve of HCCC9810 cells with METTL14^{R298H}, METTL14^{wt}, or negative control (n=3). **(I)** Colony formation assay of HCCC9810 cells with METTL14^{R298H}, METTL14^{wt}, or negative control. The number of colonies were counted and presented in the histogram (n=3). **(J)** Representative images (left) and quantification (right) of transwell migration and invasion assays in HCCC9810 cells with METTL14^{wt}, METTL14^{R298H}, or negative control (n=3). **(K)** Wound healing assay in RBE and HCCC9810 cells with METTL14^{R298H}, METTL14^{wt}, or negative control (n=3). **(L)** Representative images (left) and quantification (right) of EDU assays in RBE and HCCC9810 cells with METTL14^{wt}, METTL14^{R298H}, or negative control (n=3). The P values were calculated using unpaired two-sided Student's t test with no correction for multiple comparison. Data are shown as mean ± SEM. *P < 0.05, **P < 0.01, ***P < 0.001; R298H, METTL14^{R298H}; WT, METTL14^{wt}; NC, negative control.



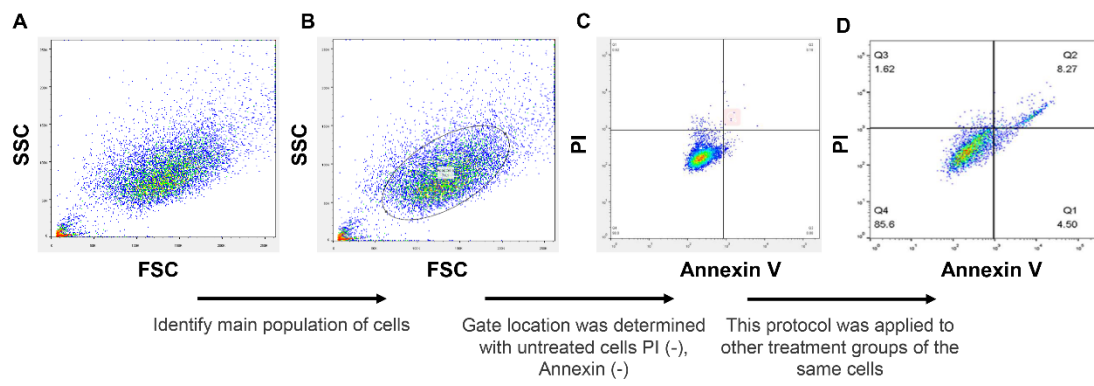
Supplementary.Fig.4 (A) Apoptotic assay of HCCC9810 cells with METTL14^{R298H}, METTL14^{wt}, or negative control were determined by a PI and annexin V double-staining assay and analysis by flow cytometry (n=3). **(B)** GGAC is the most common m⁶A motif significantly enriched in the m⁶A peaks, and the m⁶A peaks are especially

enriched in the vicinity of the stop codon. **(C)** Gene plots of MACF1 coding region harboring m6A peaks. Coverage of IP and input control is indicated in red and blue, respectively. The blue boxes in the bottom panel represent exons and UTRs. **(D)** RNA lifetime for MACF1 in HCCC9810 cells transfected with METTL14^{R298H}, METTL14^{wt}, or negative control. **(E)** The m⁶A modification level of MACF1 was validated in methylated RNA Immunoprecipitation (MeRIP) (n=3). **(F)** Immunoprecipitation of METTL14-related RNA in NC, METTL14^{wt} and METTL14^{R298H} was conducted followed by RT-qPCR to detect the amount of MACF1 mRNA binding to METTL14 (n=3). **(G)** Upregulated MACF1 mRNA expression was detected in 66 pairs of CCA tumor tissues by qRT-PCR ($p < 0.001$). **(H)** Representative images of MACF1 immunofluorescence in METTL14^{wt} and METTL14^{R298H} containing in HCCC9810 cells. All data are representative of at least two independent experiments with similar results. **(I)** The bar plot shows the MACF1 foci number in the METTL14 positive cells (n=3). **(J)** MACF1 mRNA expression in METTL14^{wt} and METTL14^{R298H} in RBE and HCCC9810 cell lines (n=3). **(K)** The knockdown efficiency of MACF1 in RBE and HCCC9810 cell lines was tested by western blot analysis. **(L)** Knockdown of MACF1 in RBE and HCCC9810 cells by siRNA were verified by qRT-PCR (n=3). The P values were calculated using unpaired two-sided Student's t test with no correction for multiple comparison. Data are shown as mean \pm SEM. *P < 0.05, **P < 0.01, ***P < 0.001; R298H, METTL14^{R298H}; WT, METTL14^{wt}; NC, negative control.

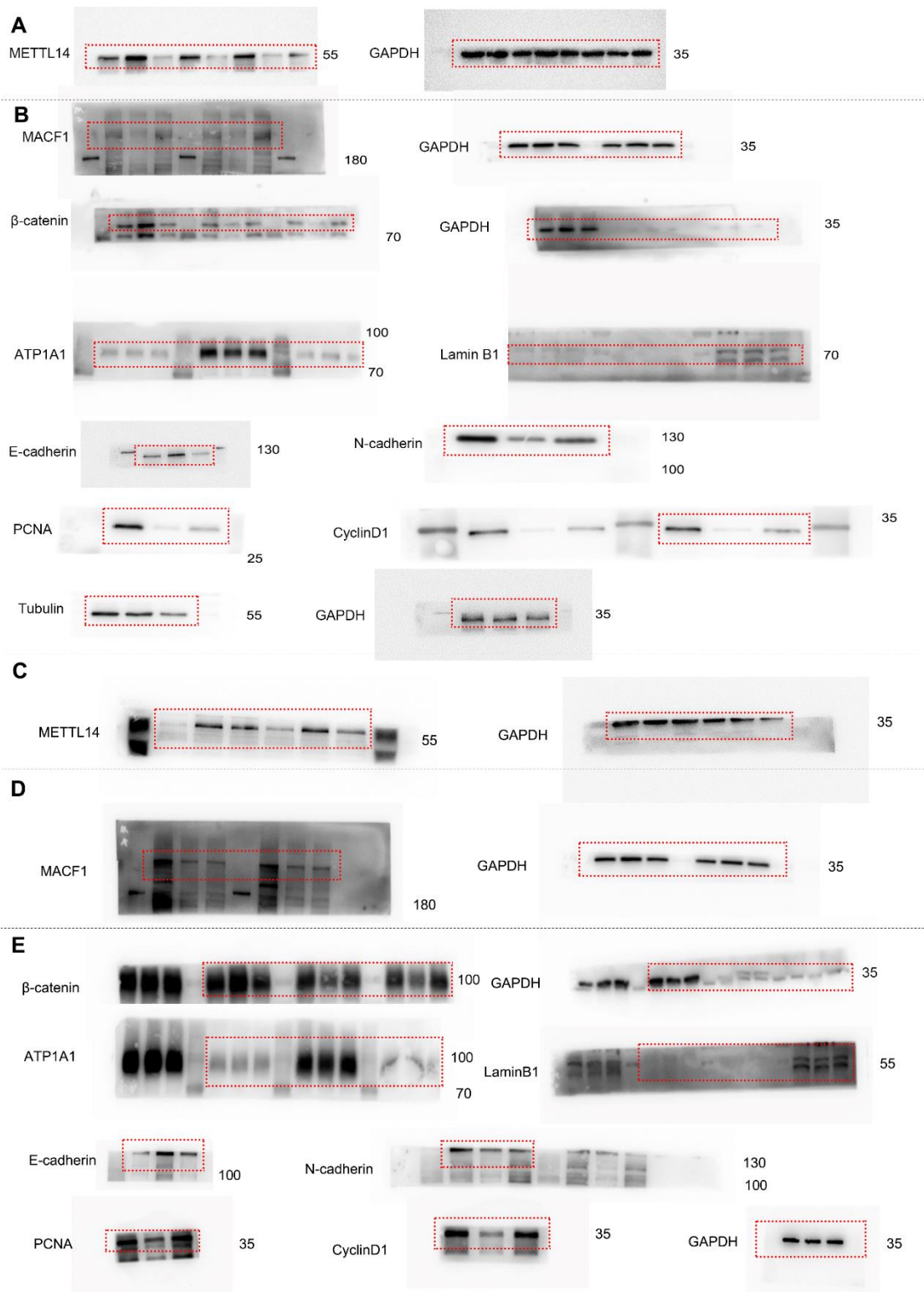


Supplementary Fig.5 **(A)** Colony formation assay of HCCC9810 cells with negative control and MACF1-siRNA (n=3). **(B)** Apoptotic assay of HCCC9810 cells with negative control and MACF1-siRNA were determined by a PI and annexin V double-staining assay and analysis by flow cytometry (n=3). **(C)** Proliferation curve of

HCCC9810 cells with negative control and MACF1-siRNA (n=3). **(D)** Representative images (left) and quantification (right) of transwell migration and invasion assays in HCCC9810 cells with negative control and MACF1-siRNA (n=3). **(E)** Wound healing assay in RBE and HCCC9810 cells with negative control and MACF1-siRNA (n=3). **(F)** Representative images (left) and quantification (right) of EDU assays in RBE and HCCC9810 cells with negative control and MACF1-siRNA (n=3). **(G)** Western blot analysis was performed to analyze the expression of β -catenin in the cytoplasmic, membrane and nuclear extracts in HCCC9810 cells. All data are representative of at least two independent experiments with similar results. **(H)** Representative images of β -catenin immunofluorescence showed nuclear β -catenin tended to be increased by expression of METTL14^{R298H} compared to METTL14^{wt} in HCCC9810 cells. **(I)** MACF1 siRNA transfected in METTL14^{R298H}-overexpressing cells, and the representative images of nucleus translocation of β -catenin is shown using immunofluorescence. The P values were calculated using unpaired two-sided Student's t test with no correction for multiple comparison. Data are shown as mean \pm SEM. *P < 0.05, **P < 0.01, ***P < 0.001; R298H, METTL14^{R298H}; WT, METTL14^{wt}; NC, negative control.



Supplementary Fig.6 FACS Gating strategy for tumor cells



Supplementary Fig. 7 (A) Uncropped scans from Fig. 4. (B) Uncropped scans from Fig. 5. (C) Uncropped scans from Supplementary Fig. 3. (D) Uncropped scans from Supplementary Fig. 4. (E) Uncropped scans from Supplementary Fig. 5.

Supplementary Table 1. General Description of Patients with CCA from Nanjing Medical University

	Total	iCCA	pCCA
Age			
Mean (SD)	61.0 (± 9.3)	60.1 (± 9.0)	61.5 (± 9.6)
Gender			
Male	45 (67.2%)	16 (66.7%)	29 (67.4%)
Female	22 (32.8%)	8 (33.3%)	14 (32.6%)
HBV			
Yes	15 (22.4%)	8 (33.3%)	7 (16.3%)
No	51 (76.1%)	16 (66.7%)	35 (81.4%)
N/A	1 (1.5%)	0 (0.0%)	1 (2.3%)
Stage			
I	11 (16.4%)	7 (29.2%)	4 (9.3%)
II	20 (29.9%)	6 (25.0%)	14 (32.6%)
III	18 (26.9%)	1 (4.2%)	17 (39.5%)
IV	18 (26.9%)	10 (41.7%)	8 (18.6%)

NMU: Nanjing Medical University; CCA: cholangiocarcinoma; SD: Standard Deviation; HBV: Hepatitis B virus.

Supplementary Table 2. Summary of exome sequencing results

	Total	iCCA	pCCA
Tumor/normal pair sequenced			
Tumor depth Mean (SD)	94.4 (± 11.1)	96.9 (± 10.4)	93.0 (± 11.3)
Normal depth Mean (SD)	91.8 (± 11.5)	94.1 (± 11.1)	90.5 (± 11.6)
Pool			
Tumor/normal pair sequenced (mean)			
SNV	84587/112.5	66508/113	18079/112
INDEL	7408/10.5	5329/5	2079/16

NMU: Nanjing Medical University; CCA: cholangiocarcinoma; SNV: Single Nucleotide Variant; INDEL: Insertion and deletion.

Supplementary Table 3. Copy number burden analysis results based on TitanCNA somatic copy number

CNV Type	Median CNAB of pCCA	Median CNAB of iCCA	P*
All Burden	3.91%	17.32%	7.98E-04
Amplification Burden	0.55%	7.50%	1.90E-06
Deletion Burden	1.84%	9.34%	4.34E-02

* P value of Wilcoxon rank sum test

Supplementary Table 4. Proportion of COSMIC liver specific signatures

Signature	pCCA		iCCA	
	HBV	non-HBV	HBV	non-HBV
Signature 12	2.03%	0.24%	7.61%	0.10%
Signature 16	3.95%	0.00%	7.76%	3.72%
Signature 24	0.00%	0.00%	10.65%	0.00%
All Signature Liver	5.98%	0.24%	26.02%	3.82%

Supplementary Table 5. Proportion of COSMIC 30 mutation signatures.

Signature	pCCA	iCCA	All
Signature 1	44.71%	27.19%	30.89%
Signature 6	27.52%	21.93%	23.11%
Signature 4	3.73%	10.13%	8.78%
Signature 22	2.37%	9.96%	8.35%
Signature 15	4.47%	2.62%	3.01%
Signature 9	3.05%	3.58%	3.47%
Signature 8	6.41%	0.00%	1.35%
Signature 13	3.84%	1.88%	2.30%
Signature 16	0.00%	4.50%	3.55%
Signature 3	0.00%	4.26%	3.36%
Signature 2	2.64%	1.17%	1.48%
Signature 12	0.63%	2.04%	1.74%
Signature 7	0.44%	2.17%	1.81%
Signature 10	0.00%	2.44%	1.92%
Signature 26	0.00%	2.20%	1.73%
Signature 24	0.00%	2.16%	1.71%
Signature 11	0.00%	0.82%	0.65%
Signature 29	0.00%	0.63%	0.50%
Signature 17	0.14%	0.20%	0.19%
Signature 21	0.00%	0.12%	0.10%
Signature 27	0.02%	0.00%	0.00%
Signature 28	0.02%	0.00%	0.00%
Signature 5	0.00%	0.00%	0.00%
Signature 25	0.00%	0.00%	0.00%
Signature 30	0.00%	0.00%	0.00%
Signature 20	0.00%	0.00%	0.00%
Signature 23	0.00%	0.00%	0.00%
Signature 18	0.00%	0.00%	0.00%
Signature 14	0.00%	0.00%	0.00%
Signature 19	0.00%	0.00%	0.00%

Supplementary Table 6. Prognostic effect of copy number burden based on TitanCNA somatic copy number adjusted for tumor purity.

Type	HR	MS L	MS H	P*
pCCA	2.89	-	404	3.63E-02
iCCA	0.84	600	420	4.52E-01

MS L/H: Median survival time of low/high CNAB subgroup

* P value of Cox Proportional-Hazards model adjusted for age, gender, tumor stage and HBV status.

Supplementary Table 7. Curated significantly mutated genes.

Gene	Recurrent mutation	All	iCCA	pCCA	ratio	Subtype specific	class
<i>TP53</i>	1	28.45%	32.18%	17.24%	1.87		Report
<i>KRAS</i>	1	18.39%	19.16%	16.09%	1.19		Report
<i>ARID1A</i>	0	7.18%	8.43%	3.45%	2.44	iCCA	Report
<i>SMAD4</i>	1	6.32%	6.51%	5.75%	1.13		Report
<i>PBRM1</i>	1	5.75%	6.90%	2.30%	3	iCCA	Report
<i>NF1</i>	0	5.75%	4.98%	8.05%	0.62		Report
<i>MACF1</i>	0	5.17%	6.13%	2.30%	2.67	iCCA	New
<i>GNAS</i>	1	5.17%	4.21%	8.05%	0.52		Report
<i>PIK3CA</i>	1	4.89%	5.36%	3.45%	1.56		Report
<i>EPHA2</i>	0	4.60%	5.36%	2.30%	2.33	iCCA	New
<i>BAP1</i>	0	4.60%	4.98%	3.45%	1.44		Report
<i>ARID2</i>	1	4.02%	4.60%	2.30%	2	iCCA	Report
<i>IDH1</i>	1	3.74%	4.98%	0.00%	#DIV/0!	iCCA	Report
<i>ATM</i>	0	3.45%	3.45%	3.45%	1		New
<i>PTEN</i>	1	3.45%	4.21%	1.15%	3.67	iCCA	Report
<i>RBM10</i>	0	3.16%	1.92%	6.90%	0.28	pCCA	New
<i>APC</i>	0	3.16%	3.07%	3.45%	0.89		Report
<i>STK11</i>	0	3.16%	2.68%	4.60%	0.58		Report
<i>RB1</i>	0	2.87%	3.45%	1.15%	3	iCCA	Report
<i>TGFBR2</i>	0	2.87%	2.30%	4.60%	0.5	pCCA	Report
<i>PIK3R1</i>	0	2.59%	1.92%	4.60%	0.42	pCCA	New
<i>BRAF</i>	1	2.59%	3.07%	1.15%	2.67	iCCA	Report
<i>ERBB2</i>	1	2.59%	2.30%	3.45%	0.67		Report
<i>NRAS</i>	1	2.30%	2.68%	1.15%	2.33	iCCA	Report
<i>MLLT4</i>	0	2.01%	2.30%	1.15%	2	iCCA	New
<i>BRCA2</i>	0	2.01%	1.92%	2.30%	0.83		New
<i>SLC8A1</i>	1	2.01%	2.30%	1.15%	2	iCCA	Report
<i>TGFBR1</i>	1	2.01%	1.92%	2.30%	0.83		Report
<i>NACC1</i>	0	1.72%	1.15%	3.45%	0.33	pCCA	New
<i>ELF3</i>	0	1.72%	1.15%	3.45%	0.33	pCCA	Report
<i>SMARCA4</i>	0	1.44%	1.53%	1.15%	1.33		New
<i>WHSC1</i>	0	1.44%	1.53%	1.15%	1.33		New
<i>CTNNB1</i>	1	1.15%	1.15%	1.15%	1		Report
<i>METTL14</i>	1	0.86%	0.38%	2.30%	0.17	pCCA	New
<i>AXIN1</i>	0	0.86%	1.15%	0.00%	#DIV/0!		New
<i>CDKN2A</i>	0	0.86%	0.77%	1.15%	0.67		Report

Supplementary Table 8. Frequently altered focal CNA regions.

	Type	Cytoband	Original Somatic Copy number						Genes	Purity-adjusted Somatic Copy number					
			Peak Limits	Gistic2 Q value	CCA	iCCA	pCCA	P*		Peak Limits	Gistic2 Q value	CCA	iCCA	pCCA	P*
Peak 1	Amp	1q21.3	chr1:15288421-153028730	9.98E-05	50.30%	59.52%	23.26%	4.11E-05	<i>S100A7</i>	chr1:152136817-152998692	4.08E-04	44.38%	54.76%	13.95%	7.83E-05
Peak 2	Amp	3q29	chr3:195505680-195512202	2.35E-01	27.22%	26.98%	27.91%	1.00E+00	<i>BCL6/EIF4A2/ETV5/MECOM/LPP/MLF1/MUC4/PIK3CA/SOX2/TFRC/TP63/GMPS/MAP3K13/IGF2BP2/TBLIXR1/MB21D2/MUC4</i>	chr3:194946409-195800811	6.53E-01	23.08%	23.02%	23.26%	5.46E-01
Peak 3	Amp	5p15.33	chr5:712602-833506	1.01E-01	31.95%	37.30%	16.28%	1.32E-02	<i>SDHA</i>	chr5:1094389-3513533	6.47E-01	30.77%	37.30%	11.63%	6.86E-03
Peak 4	Amp	7q31.2	chr7:116201362-117003338	5.23E-03	26.63%	30.95%	13.95%	2.97E-02	<i>MET</i>	chr7:115576366-118760185	1.41E-02	27.81%	32.54%	13.95%	2.85E-02
Peak 5	Amp	8q24.21	chr8:127569976-130496004	6.22E-02	51.48%	61.11%	23.26%	1.83E-05	<i>MYC/NDRG1/FAM135B</i>	chr8:127272502-129436179	1.82E-06	51.48%	61.11%	23.26%	1.83E-05
Peak 6	Amp	12q15	chr12:69784665-70048359	7.76E-17	24.26%	22.22%	30.23%	3.07E-01	<i>MDM2</i>	chr12:68956086-70496201	2.47E-15	22.49%	21.43%	25.58%	2.99E-01
Peak 7	Amp	13q33.3	chr13:108519278-108881202	1.70E-01	18.93%	19.84%	16.28%	8.22E-01	<i>ERCC5/GPC5/SOX21</i>	chr13:96120780-115169878	1.50E-01	23.67%	25.40%	18.60%	6.44E-01
Peak 8	Amp	17q12	chr17:37763071-37900028	1.62E-02	22.49%	21.43%	25.58%	6.73E-01	<i>ERBB2/CDK12</i>	chr17:37728462-37815781	4.97E-01	19.53%	19.84%	18.60%	5.25E-01
Peak 9	Amp	19q12	chr19:30205961-30934085	5.41E-03	20.71%	22.22%	16.28%	5.15E-01	<i>CCNE1</i>	chr19:30985893-41377687	2.34E-02	20.71%	19.05%	25.58%	5.18E-01
Peak 10	Del	1p36.13	chr1:16975100-17019152	8.63E-09	44.97%	47.62%	37.21%	2.88E-01	<i>SDHB</i>	chr1:1-29605264	1.15E-10	40.24%	46.03%	23.26%	7.80E-02
Peak 11	Del	2p24.1	chr2:21362860-23608429	1.68E-01	11.83%	9.52%	18.60%	1.68E-01	<i>DNMT3A/NCOA1/C2orf44/ASXL2/BCL6/EIF4A2/ETV5/MECOM/LPMLF1/MUC4/PIK3CA/SOX2/TFRC/</i>	chr2:1520676-23986790	5.89E-01	8.28%	5.56%	16.28%	4.10E-02
Peak 12	Del	3q29	chr3:195460176-195686566	2.16E-01	10.65%	12.70%	4.65%	1.65E-01		chr3:195049593-195800811	6.92E-01	10.06%	11.11%	6.98%	4.11E-01

Peak 13	Del	4q35.2	chr4:18639246 5-191154276	4.21E-02	42.60%	49.21%	23.26%	3.97E-03	<i>TP63/GMPS/MAP3K13/IGF2BP2</i> / <i>TBL1XR1/MB21D2/MUC4</i>	<i>CASP3/FAT1</i>	chr4:163196244- 191154276	1.81E-02	36.09%	41.27%	20.93%	3.97E-03
Peak 14	Del	5q14.2	chr5:79852637 -81679260	1.34E-01	32.54%	33.33%	30.23%	8.51E-01	<i>PIK3RI/RAD17</i>	chr5:64080559- 113260791	6.66E-03	31.36%	31.75%	30.23%	8.48E-01	
Peak 15	Del	7q35	chr7:14397914 1-144094614	2.46E-01	11.24%	11.90%	9.30%	7.84E-01	<i>EZH2/MNX1/FAM131B/</i> <i>CNTNAP2/KMT2C</i>	<i>CDKN2A</i>	chr9:21942244- 22867276		13.02%	12.70%	13.95%	7.85E-01
Peak 16	Del	9p21.3	chr9:21931171 -21993843	4.70E-09	51.48%	53.17%	46.51%	4.83E-01	<i>FAS/BMPR1A/CYP2C8/FGFR2</i> / <i>TLX1/MGMT/NFKB2/PTEN/</i> <i>TCF7L2/CPEB3/NT5C2/SUFU/</i> <i>VTIIA/KIAA1598/FAM22A</i> <i>BIRC3/ATM/CBL/DDX6/MLL/</i> <i>DDX10/FLII/KCNJ5/PAFAH1B2/</i> <i>POU2AF1/SDHD/ZBTB16/</i> <i>ARHGEF12/MAML2/FAT3/</i> <i>BCL9L/FOXRI</i>	chr10:89788322- 135534747	4.23E-02	50.89%	52.38%	46.51%	4.83E-01	
Peak 17	Del	10q25.2	chr10:1122114 48-114192711	1.03E-01	31.95%	34.92%	23.26%	1.87E-01	<i>POLE</i>	chr11:97903454- 135006516	1.04E-03	28.99%	30.95%	23.26%	8.48E-01	
Peak 18	Del	11q23.3	chr11:1088114 65-116619582	1.85E-01	25.44%	29.37%	13.95%	6.66E-02	<i>PER1/TP53/YWHAE/GAS7/</i> <i>USP6/RABEP1</i>	chr12:84949118- 133851895	1.81E-02	22.49%	26.98%	9.30%	6.64E-02	
Peak 19	Del	12q24.33	chr12:1322132 85-133851895	4.67E-03	23.67%	23.81%	23.26%	1.00E+00	<i>BCL2/DCC/KDSR/SMAD4/MALT</i> 1	chr17:1- 11704306	2.91E-04	23.08%	24.60%	18.60%	8.35E-01	
Peak 20	Del	17p13.3	chr17:1- 4017349	1.90E-01	42.60%	42.86%	41.86%	1.00E+00	<i>ZNF429</i>	chr18:42889427- 64009795	9.13E-02	43.79%	46.03%	37.21%	1.00E+00	
Peak 21	Del	18q21.2	chr18:4819054 9-49867515	5.18E-02	39.05%	34.92%	51.16%	7.11E-02		chr19:20064879- 20311900	1.12E-05	36.09%	33.33%	44.19%	1.46E-01	
Peak 22	Del	19p12	chr19:2237967 6-22836478	4.89E-02	25.44%	29.37%	13.95%	6.66E-02			6.31E-01	41.42%	49.21%	18.60%	6.66E-02	

Amp: Amplification; Del: Deletion; *: P value of frequency difference test.

Supplementary Table 9. Curated recurrent mutations

Hugo Symbol	Entrez Gene Id	Chromosome	Start position	End position	Variant Classification	Variant Type	Allele1	Allele2	Sample	cDNA Change	Protein Change	SIFT	CADD	Polyphen2	GERP
<i>ROBO1</i>	6091	3	78766504	78766504	Nonsense Mutation	SNP	C	A	D70036-115	c.838G>T	p.E280*	.	38	.	5.54
<i>ROBO1</i>	6091	3	78766504	78766504	Nonsense Mutation	SNP	C	A	DO222541	c.838G>T	p.E280*	.	38	.	5.54
<i>PTEN</i>	5728	10	89692905	89692905	Missense Mutation	SNP	G	A	D70036-73	c.389G>A	p.R130Q	.	36	0.998	5.22
<i>PTEN</i>	5728	10	89692905	89692905	Missense Mutation	SNP	G	A	DO222603	c.389G>A	p.R130Q	.	36	0.998	5.22
<i>PIK3CA</i>	5290	3	178936091	178936091	Missense Mutation	SNP	G	A	D70036-41	c.1633G>A	p.E545K	0.25	36	0.909	5.78
<i>PIK3CA</i>	5290	3	178936091	178936091	Missense Mutation	SNP	G	A	DO222442	c.1633G>A	p.E545K	0.25	36	0.909	5.78
<i>PIK3CA</i>	5290	3	178936091	178936091	Missense Mutation	SNP	G	A	DO222443	c.1633G>A	p.E545K	0.25	36	0.909	5.78
<i>PIK3CA</i>	5290	3	178936091	178936091	Missense Mutation	SNP	G	A	DO222892	c.1633G>A	p.E545K	0.25	36	0.909	5.78
<i>SPTAN1</i>	6709	9	131378011	131378011	Missense Mutation	SNP	G	A	D70036-37	c.5234G>A	p.R1745H	0.05	35	0.999;0.991;0.995	5.71
<i>SPTAN1</i>	6709	9	131378011	131378011	Missense Mutation	SNP	G	A	DO222955	c.5234G>A	p.R1745H	0.05	35	0.999;0.991;0.995	5.71
<i>VASH2</i>	79805	1	213134569	213134569	Missense Mutation	SNP	C	T	D70036-61	c.338C>T	p.A113V	0.16	34	0.868;0.996;0.994	4.98
<i>METTL14</i>	57721	4	119626803	119626803	Missense Mutation	SNP	G	A	D70036-37	c.893G>A	p.R298H	0.01	28.7	1.0;1.0	4.98
<i>METTL14</i>	57721	4	119626803	119626803	Missense Mutation	SNP	G	A	DO222817	c.893G>A	p.R298H	0.01	28.7	1.0;1.0	4.98
<i>RNF150</i>	57484	4	141868808	141868808	Splice_Site	SNP	C	T	D70036-25	c.890G>A	p.R297Q	.	28.6	0.951;0.726;0.957	5.11
<i>RNF150</i>	57484	4	141868808	141868808	Splice_Site	SNP	C	T	SRR1535216	c.890G>A	p.R297Q	.	28.6	0.951;0.726;0.957	5.11
<i>TGFBR1</i>	7046	9	101891287	101891287	Missense Mutation	SNP	C	T	LD8k0723	c.248C>T	p.P83L	0	28.3	1.0;0.995;0.039	6.08
<i>TGFBR1</i>	7046	9	101891287	101891287	Missense Mutation	SNP	C	T	DO222852	c.248C>T	p.P83L	0	28.3	1.0;0.995;0.039	6.08
<i>NRXN3</i>	9369	14	79181293	79181293	Missense Mutation	SNP	C	T	D70036-37	c.736C>T	p.R246C	.	26.7	0.999;0.886	5.07
<i>NRXN3</i>	9369	14	79181293	79181293	Missense Mutation	SNP	C	T	DO222439	c.736C>T	p.R246C	.	26.7	0.999;0.886	5.07
<i>SEC24C</i>	9632	10	75523303	75523303	Missense Mutation	SNP	G	T	D70036-69	c.1043G>T	p.G348V	0.32	24	0.757;0.644;0.546	5.51
<i>SEC24C</i>	9632	10	75523303	75523303	Missense Mutation	SNP	G	T	DO222740	c.1043G>T	p.G348V	0.32	24	0.757;0.644;0.546	5.51
<i>CTNNB1</i>	1499	3	41266124	41266124	Missense Mutation	SNP	A	G	D70036-87	c.121A>G	p.T41A	0	23.7	0.694	5.91
<i>CTNNB1</i>	1499	3	41266124	41266124	Missense Mutation	SNP	A	G	DO222973	c.121A>G	p.T41A	0	23.7	0.694	5.91
<i>VASH2</i>	79805	1	213134569	213134569	Missense Mutation	SNP	C	A	DO222983	c.338C>A	p.A113E	0.04	23.5	0.987;0.999;0.998	4.98
<i>SLC8A1</i>	6546	2	40656129	40656129	Missense Mutation	SNP	C	T	D70036-49	c.1292G>A	p.R431H	0.01	21.5	0.999;0.999;0.999;1.0;0.999	6.17
<i>SLC8A1</i>	6546	2	40656129	40656129	Missense Mutation	SNP	C	T	DO222952	c.1292G>A	p.R431H	0.01	21.5	0.999;0.999;0.999;1.0;0.999	6.17

<i>ERBB2</i>	2064	17	37879658	37879658	Missense Mutation	SNP	G	A	D70036-41	c.2033G>A	p.R678Q	0.07	20.2	0.103;0.02;0.103	4.97
<i>ERBB2</i>	2064	17	37879658	37879658	Missense Mutation	SNP	G	A	DO222574	c.2033G>A	p.R678Q	0.07	20.2	0.103;0.02;0.103	4.97
<i>ZNF354A</i>	6940	5	178140425	178140425	Frame Shift_Del	DEL	T	-	D70036-87	c.454delA	p.I152fs				
<i>ZNF354A</i>	6940	5	178140425	178140441	Frame Shift_Del	DEL	TTTTTTGTGGGTGGCT	-	SRR1535082 c.438_454delAGCCACCCACAAAAAAA p.ATHKKI147fs						
<i>WDTCI</i>	23038	1	27621107	27621108	Frame Shift_Ins	INS	-	G	D70036-87	c.860_861insG	p.MG287fs				
<i>WDTCI</i>	23038	1	27621107	27621108	Frame Shift_Ins	INS	-	G	DO222905	c.860_861insG	p.MG287fs				
<i>WASF3</i>	10810	13	27255387	27255387	Frame Shift_Del	DEL	C	-	D70036-51	c.913delC	p.P310fs				
<i>WASF3</i>	10810	13	27255387	27255387	Frame Shift_Del	DEL	C	-	D70036-87	c.913delC	p.P310fs				
<i>TAP2</i>	6891	6	32805788	32805788	Frame Shift_Del	DEL	G	-	D70036-05	c.223delC	p.L75fs				
<i>TAP2</i>	6891	6	32805788	32805788	Frame Shift_Del	DEL	G	-	D70036-37	c.223delC	p.L75fs				
<i>RPL22</i>	6146	1	6257785	6257785	Frame Shift_Del	DEL	T	-	D70036-05	c.44delA	p.K16fs				
<i>RPL22</i>	6146	1	6257785	6257785	Frame Shift_Del	DEL	T	-	LD8k4455	c.44delA	p.K16fs				
<i>RABL6</i>	55684	9	139734212	139734212	Frame Shift_Del	DEL	C	-	D70036-05	c.1825delC	p.P612fs				
<i>PHLDA1</i>	22822	12	76424936	76424940	Frame Shift_Del	DEL	GTTGC	-	LD8k4465	c.582_586delGCAAC	p.QQQ194fs				
<i>PHLDA1</i>	22822	12	76424936	76424940	Frame Shift_Del	DEL	GTTGC	-	D70036-99	c.582_586delGCAAC	p.QQQ194fs				
<i>LARP4B</i>	23185	10	890939	890939	Frame Shift_Del	DEL	T	-	LD8k4455	c.487delA	p.T163fs				
<i>LARP4B</i>	23185	10	890939	890939	Frame Shift_Del	DEL	T	-	D70036-87	c.487delA	p.T163fs				
<i>KMT2A</i>	4297	11	118344185	118344186	Frame Shift_Ins	INS	-	C	LD8k4455	c.2311_2312insC	p.T771fs				
<i>KMT2A</i>	4297	11	118344185	118344186	Frame Shift_Ins	INS	-	C	DO222427	c.2311_2312insC	p.T771fs				
<i>KLF3</i>	51274	4	38691475	38691476	Frame Shift_Ins	INS	-	C	D70036-99	c.670_671insC	p.S224fs				
<i>KLF3</i>	51274	4	38691475	38691476	Frame Shift_Ins	INS	-	C	DO222913	c.670_671insC	p.S224fs				
<i>GRINA</i>	2907	8	145065478	145065479	Frame Shift_Ins	INS	-	C	DO222454	c.87_88insC	p.P30fs				
<i>DDX5</i>	1655	17	62500099	62500102	Splice Site	DEL	ACAG	-	D70036-87	c.440_442delCTGT	p.SV147fs				
<i>DDX5</i>	1655	17	62500099	62500099	Splice Site	ONP	ACAG	ACAG	DO222955						
<i>CCDC116</i>	164592	22	21989446	21989446	Frame Shift_Del	DEL	C	-	LD8k4455	c.1094delC	p.S365fs				
<i>CCDC116</i>	164592	22	21989446	21989446	Frame Shift_Del	DEL	C	-	D70036-87	c.1094delC	p.S365fs				

<i>BCL9</i>	607	1	147091500	147091501	Frame Shift_Ins	INS	-	C	LD8k4455	c.1539_1540insC	p.P514fs
<i>BCL9</i>	607	1	147091500	147091501	Frame Shift_Ins	INS	-	CC	DO222427	c.1539_1540insCC	p.P514fs
<i>ATP8B1</i>	5205	18	55365039	55365040	Frame Shift_Ins	INS	-	T	D70036-05	c.614_615insA	p.N205fs
<i>ATP8B1</i>	5205	18	55365039	55365040	Frame Shift_Ins	INS	-	T	D70036-99	c.614_615insA	p.N205fs
<i>ATF7IP</i>	55729	12	14577801	14577802	Frame Shift_Ins	INS	-	A	D70036-05	c.952_953insA	p.E318fs
<i>ATF7IP</i>	55729	12	14577801	14577802	Frame Shift_Ins	INS	-	A	D70036-99	c.952_953insA	p.E318fs

SNP: single nucleotide polymorphism; DEL: Deletion; INS: Insertion; SIFT: Sorting Intolerant from Tolerant; CADD: Combined Annotation-Dependent Depletion; GERP: Genomic Evolutionary Rate Profiling

